Award Accounts

The Chemical Society of Japan Award for Creative Work for 2010

Novel Developed Systems and Techniques Based on Double-Network Principle

Zi Liang Wu,[1] Takayuki Kurokawa,[2,3] and Jian Ping Gong*[2]

[1]Division of Biological Sciences, Graduate School of Science, Hokkaido University, Sapporo 060-0810

[2]Faculty of Advanced Life Science, Graduate School of Science, Hokkaido University, Sapporo 060-0810

[3]Creative Research Initiative Sousei, Hokkaido University, Sapporo 001-0021

Received July 1, 2011; E-mail: gong@mail.sci.hokudai.ac.jp

The double-network hydrogels (DN gels), developed by our group in 2003, have attracted increasing attention due to their excellent mechanical performance and unique fracture mechanism. The anomalously large fracture energy of DN gels up to 2200 J m^{-2} originates from the specific combination of two networks with contrasting properties. The first brittle network serves as *sacrificial bonds*, which breaks into small clusters to efficiently disperse the stress around the crack tip into the surrounding damage zone, while the second ductile polymer chains act as *hidden length*, which extends extensively to sustain large deformation. The DN gels also exhibit good biocompatibility and low friction resistance. Owing to these superior properties, DN gels possess promising prospective in industrial and medicine fields, especially for load-bearing artificial soft tissues such as artificial cartilage. However, there are several critical problems limiting the practical applications of DN gels, such as how to produce tough artificial tissue with complex shapes or bond a gel to a solid substrate. To address these specific issues, we have developed new systems and techniques based on the DN principle. These achievements, including synthesis of ultrathin DN gels, bonding of one gel to another gel or solid substrate, free-shaping of DN gels, enhancing typical single network gels by creating a DN structure, will be briefly introduced in this account paper. We believe that these new techniques will substantially promote the practical applications of DN hydrogels and extent the DN principle to other systems.

1. Introduction

Hydrogels, a typical soft and wet matter, consist of cross-linked polymers and a large amount of water. Owing to their stimuli-response capability, high permeability to small molecules, and similarity to soft biotissues, hydrogels show promising applications in soft robotics, molecular filters, drug delivery, scaffolds for cell culture, and tissue engineering.[1–9] Compared with natural hydrogels such as cartilage, tendon, and muscle, the conventional hydrogels lack sufficient mechanical strength that greatly limits their extensive applications in mechanical devices, soft actuators, and artificial tissues.[10] For example, cartilage, containing 75 wt% water, possesses a compressive fracture stress of 36 MPa, allowing it to sustain a daily compression of several MPa.[11–13] The tearing energy, T, defined as the work required in creating a unit area of fracture surface, of common hydrogels fall in a range of 0.1–1 J m^{-2}, much smaller than that of cartilage, 100–1000 J m^{-2}.[14–18] Therefore, improving the mechanical properties of hydrogels is a critical issue to fill the gap between the synthetic and natural hydrogels, and to expand their applications in load-bearing systems.

In recent years, there have been many efforts toward improving the strength of hydrogels,[19,20] in which several methods, i.e., slide-ring gels,[21,22] nanocomposite gels,[23,24] double-network gels,[25,26] click gel,[27,28] and tetra-PEG gels,[29] have shown good achievements. Among these hydrogels, the double-network gels (DN gels) developed by our group obtain the highest fracture stress and toughness. We attribute the outstanding mechanical performance of DN gels to the specific network structure and energy dissipation path during the deformation that will be introduced in the following part. This pioneered work of DN gels has been followed both theoretically and experimentally by many research groups.[30–44]

These gels with excellent mechanical properties show promise in load-bearing artificial tissues. However, for practical applications, we need to think of how to make the tough gels have features and properties comparable to biological tissues such as muscle with fast stimuli-response, cartilage with complex shape, ligament with tight junction to bone, or tendon with anisotropic structure. To address these critical problems, recently we developed several novel systems and techniques based on the DN principle, in terms of both the typical structure and toughening mechanism. These achievements, including

Published on the web November 19, 2011; doi:10.1246/bcsj.20110201

synthesis of ultrathin DN gels, bonding of one gel to another gel or solid porous substrate, free-shaping of DN gels, enhancing typical single network gel by creating a DN structure, should greatly expand the applications of tough hydrogels. In this account, the principle of DN gels will be generally introduced in Section **2**, and the novel developed techniques and systems will be described in Section **3**–**6**.

2. Double-Network Principle

The DN gels are generally synthesized via a two-step sequential free-radical polymerization.[25] The first step is forming a tightly crosslinked network hydrogel of polyelectrolyte. The first gel is subsequently swollen in an aqueous solution of a neutral monomer, and then the monomer is polymerized to form a loosely crosslinked, flexible network inside the first gel. This double network structure has been found effective in many combinations, if we only follow some general rules. The essential feature of DN gels is that they consist of two kinds of polymers with strong contrasting structure, as summarized below.[26]

(i) Rigid and brittle polymer as the first network, such as polyelectrolyte; soft and ductile polymer as the second network, such as neutral polymer.

(ii) The molar concentration of the second network is 20–30 times the first network.[45]

(iii) The first network is tightly while the second network is loosely crosslinked, which requires a very high molecular weight of the second polymer.

In other words, the delicate balance between a suitable brittleness of the first network and a ductility of the second network is preserved to obtain the anomalously high-strength by the DN structure. We should note here that the strongly contrasting properties of the two networks in DN gels make them quite different from conventional interpenetrated network (IPN) gels. IPN structure is usually introduced to combine various properties of each component material, such as water-absorbing ability, response to pH stimulus, and biodegradability;[46] these IPN gels do not exhibit any substantial improvement in mechanical strength to their original single network structure. The high strength of DN gels is due to a synergistic effect of the binary structure rather than a linear combination of two component networks, like conventional IPN or fiber-reinforced hydrogels.[47]

Among all the polymer pairs we studied so far, the DN gels synthesized with poly(2-acrylamido, 2-methyl-1-propanesulfonic acid) (PAMPS) polyelectrolyte as the first network and polyacrylamide (PAAm) neutral polymer as the second network stand out with unusually properties and serve as the system for our further studies. At an optimal composition, the PAMPS/PAAm DN gels show excellent mechanical performance, although they include $\approx$90 wt % water. The compressive fracture stress of the DN gels achieves several dozens of MPa, which is comparable to that of cartilage. In addition, the tearing energy reaches up to 4400 J m^{-2}, which is several thousand times of that of single network PAMPS and PAAm hydrogels.[45,48–50] It should be noted here that the tearing energy T, defined as the energy required for fracturing a unit area in a sample, was calculated by $T = 2F_{ave}/w$, where F_{ave} is the average tearing resistance force, and w is the width of the gel. The tearing energy thus defined is 2 times the fracture energy G used in our previous papers.[45,48–50]

To show the distinguished mechanical performance of the DN gels and the related toughening mechanism, we introduce here the tensile and tearing behaviors of DN gels. During the elongation tensile test, tough DN gels usually show remarkable necking phenomenon, as shown in Figure 1a. Narrowed zones appear in the sample at a certain strain, $\varepsilon \approx 2$, and increase with further elongation.[26,51–53] In the stress–strain curve, yielding occurs and a plateau region appears during the neck zone propagation, which is insensitive to strain rate. After the necking, the gel becomes very soft with an elastic modulus approximately 1/10 of that before the elongation test.[54] We confirmed that the first PAMPS network breaks into small clusters even at several percent of strain because of the intrinsic fragile properties of PAMPS single network hydrogel. These clusters play a role of physical crosslinker of long flexible PAAm chains (second PAAm network is loosely crosslinked). The fragmentation during the elongation involves dissipation, which is reflected in the hysteresis of the second loading curve (Figure 1a).[26,53,55] The necking phenomenon can be regarded as a damage accumulation of the first network; on the strongly stretched region in front of the crack tip, the gels transform into a very soft gel by breaking the first network into small clusters (Figure 1b). Both the fragmentation of PAMPS network and chain-pulling process of flexible PAAm chains from the clusters dissipate energy, endowing the DN gel with toughness. However, the former is predominant in the case of the DN gel, which is the reason why the mechanical behaviors (strength and toughness) are hardly influenced by the strain rate.[26,51,54,56]

Besides the tensile test, tearing test as a measurement of the fracture energy is applied to quantify the mechanical strength of the DN gels (Figure 2a).[50,53,57] The tearing energy T of PAMPS/PAAm DN gels ranges from 10^2 to 10^3 J m^{-2} (Figure 2c), which is 100–1000 times larger than that of single network PAAm gels ($\approx$10 J m^{-2}) or PAMPS gels ($\approx$0.1 J m^{-2}) with the similar polymer concentrations to those of DN gels. The significantly high T originates from the emergence of the large damaged zone (yielding zone) around the crack tips that has been directly observed under a color three-dimensional violet laser scanning microscope (Figure 2b).[57,58] In the fracture process of the DN gels, the stress concentrated at the crack tip efficiently causes an internal fracture of the first network around the crack tip, which remarkably dissipates energy, and therefore greatly enhances the fracture propagation resistance (Figure 2d). The internal fracture of the DN gels comes from the fragmentation of the brittle first PAMPS network, whereas the ductile PAAm chains entangled with the fractured PAMPS clusters are stretched without breaking up to a quite large extension.[26,54,56,59] Therefore, the toughening mechanism, that is, the anomalously large fracture energy of DN gels, is attributed to the necking phenomenon, whereupon the first brittle network serves as *sacrificial bonds*, which breaks into small clusters to efficiently disperse the stress around the crack tip into the surround damage zone, while the second ductile polymer chains act as *hidden length*, which extends extensively to sustain large deformation. The structure change, i.e., fragmentation of the first network, is accumulative and irreversible. Formation of large yielding or fracture zone at

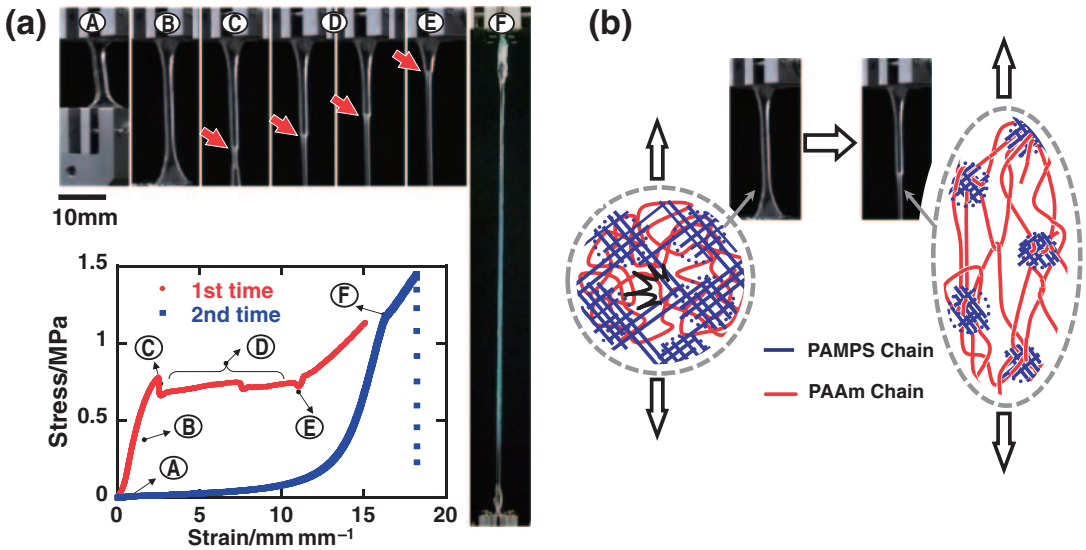

Figure 1. (a) Loading curves of PAMPS/PAAm DN gel under uniaxial elongation at a rate of 0.13 s^{-1}, and images demonstrating the necking process. The insert letters represent the correspondence between the images and the date points in the loading curves. (b) Illustration of the network structure of the DN gel before and after necking. Above a critical stress, PAMPS network fractures into clusters that behave as a sliding crosslinker of PAAm. After necking DN gel becomes soft. Reproduced with permission from Ref. 26.

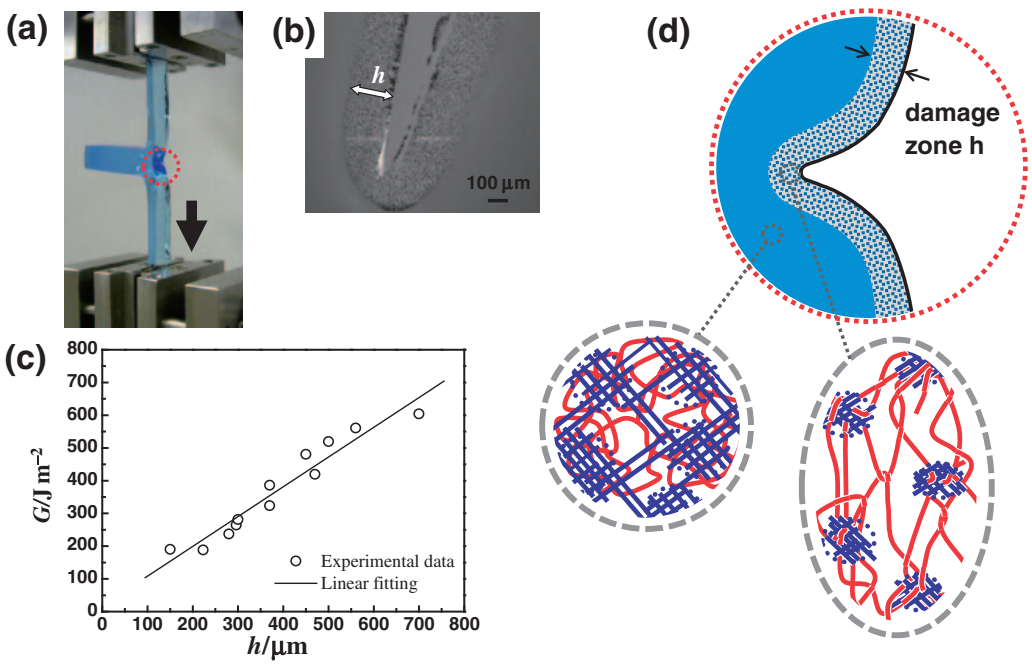

Figure 2. (a) Image of the tearing test of DN gel. (b) Image of the crack tip of the DN gel after tearing observed under a color three-dimensional violet laser scanning microscope. (c) Relationship between fracture energy, G, and the thickness of the damage zone, h. (d) Illustration of network structure at the crack front of the DN gel. It should be noted that the fracture energy G here was calculated by $G = F_{ave}/w$, where F_{ave} is the average tearing resistance force, and w is the width of the gel. The G thus calculated is one half of the tearing energy $T = 2F_{ave}/w$ conventionally used in the literature. Reproduced with permission from Ref. 26 (a and d) and Ref. 53 (b and c).

the crack tip seems to be a common feature for the tough materials, such as in the fracture of natural bones.[60]

DN gels with excellent mechanical properties also exhibit low friction resistance and suitability for regenerative medicine.[61–64] The modified DN gels show good biocompatibility and do not degrade in the in vivo environment. These characteristics make the DN gels have promising prospects in load-bearing artificial tissues. Based on the DN principle, we have developed several novel systems and techniques to produce free-shaped tough gel, to bond one gel to another gel or solid substrate, etc. that should greatly expand the applications of DN hydrogels.

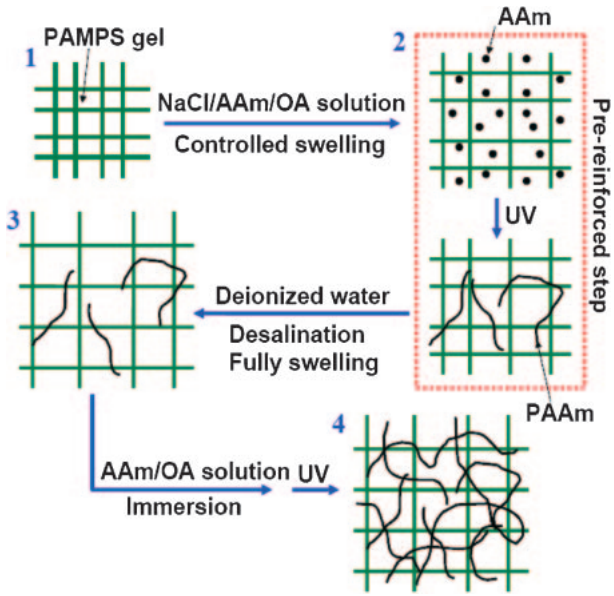

Figure 3. Synthesis procedures of the ultrathin DN gel films. Reproduced with permission from Ref. 71.

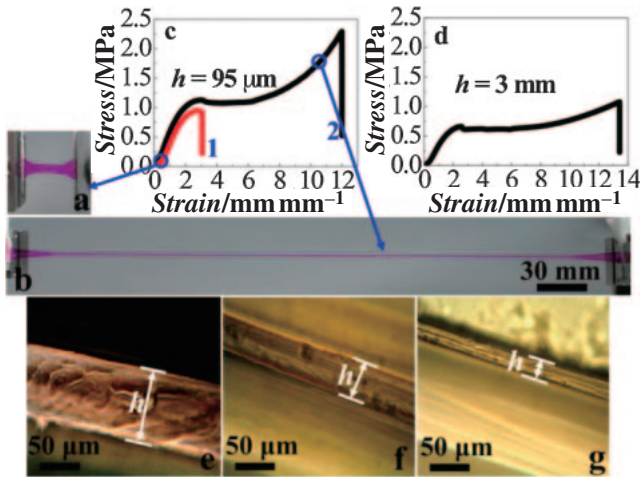

Figure 4. The UTDN gel at (a) its free-standing state and (b) the stretching state at a strain of ≈11 mm mm^{-1}, the gel was here dyed for clear visibility; (c) stress–strain curves of the pre-reinforced ultrathin film PAMPS gel (1) and the UTDN gels (thickness $h = 95\,\mu m$) (2); (d) stress–strain curve of the bulk DN gels with thickness of $h = 3$ mm; cross-section images of the UTDN gels with the thickness h of (e) ≈100, (f) ≈55, and (g) ≈30 μm obtained under phase contrast microscope. Reproduced with permission from Ref. 71.

3. Thin Film DN Gel and Its Stimuli-Responsive Behavior as Muscle

Creating soft actuators with properties comparable to human muscles, i.e., artificial muscles, is of profound interest for scientists in the research field of soft materials. The previous work mainly focused on designing materials that are strong and flexible, smartly respond to stimuli, and generate fast and high output force, to mimic the energy conversion functions observed in real muscle.[65–67] Sensing and actuating of hydrogels are usually achieved via the volume changes in response to a wide range of stimuli. Alternatively, field-induced contraction, motion, and bending of gels provide other pathways for energy conversion.[4,68–70] Even so, the weak mechanical strength and slow response are two main issues associated with the extensive use of gel-based artificial muscle.

Bulk DN gels with significantly high mechanical strength can address the above first issue.[25,26] However, the response, such as volume change, of bulk DN gels with thickness of several millimeters should be very slow. This is because the contraction kinetics of a gel is determined by cooperative diffusion, and characteristic time, τ, is related to the characteristic size of the specimen, h, $\tau \propto h^2$. Therefore, to improve the response rate, our approach is to work with ultrathin DN hydrogels.

Ultrathin PAMPS/PAAm double-network gels (UTDN gels) are synthesized by multistep photopolymerization (Figure 3),[71] adapted from the general two-step synthesis of bulk DN gel. Using two glass plates spaced with 15, 25, and 50 μm polyethylene film, we first synthesized ultrathin PAMPS gels by the first step polymerization. Then, the PAMPS gels were immersed in AAm aqueous solution containing 0.001 M initiator and 0.08 M NaCl. The introduction of salt is to prevent the PAMPS gels from dramatic swelling due to the high ionic osmotic pressure exerted on the polyelectrolyte networks. The swelling degree of the PAMPS gels in 0.08 M NaCl aqueous solution is only about half to that in pure water. In addition, the gel would be easily peeled off from the substrate in the salt solution. Following the second polymerization, PAAm chains are produced in and pre-reinforce the PAMPS gels to a level that permits us to directly manipulate the PAMPS gels at its fully swollen state in water. The following steps are similar to that in the synthesis of bulk DN gels, swelling the gel in AAm precursor solution and the third polymerization to obtain the UTDN gels.

Figure 4 shows the cross-section images of the UTDN gels after being fully swollen by water and their comparable mechanical properties to bulk DN gels. The thickness of the UTDN gel synthesized with initial space of 15–50 μm and then fully swollen in water ranges from ≈30 to ≈100 μm (Figures 4e–4g). The values of fracture stress σ_b and fracture strain ε_b of UTDN gels in tensile test are ≈2.3 MPa and ≈12 mm mm^{-1}, respectively (Figures 4a–4c). The tearing energy T is ≈1240 J m^{-2}. These mechanical performances are comparable to that of the bulk DN gels (Figure 4d). Actually, we have observed the necking phenomenon in the tensile test and damage zone at the crack tip in the tearing test, similar to that of bulk DN gels.[58] These results demonstrate the toughening mechanism of the UTDN gel is the same as that of the bulk DN gels. Therefore, the DN principle is still effective for creating strong DN gel at the microscale.

To explore the applicability of the UTDN hydrogels to artificial muscle, we have studied its solvent-triggered force generation in ethanol (EtOH) and EtOH–water mixture under a constant prestrain of 100%.[71] Figure 5a presents the cyclic changes in the isometric stress of the UTDN gels alternately triggered by water and EtOH. The magnification of one of the cycles (800–1300 s) is shown in Figure 5b. When the UTDN

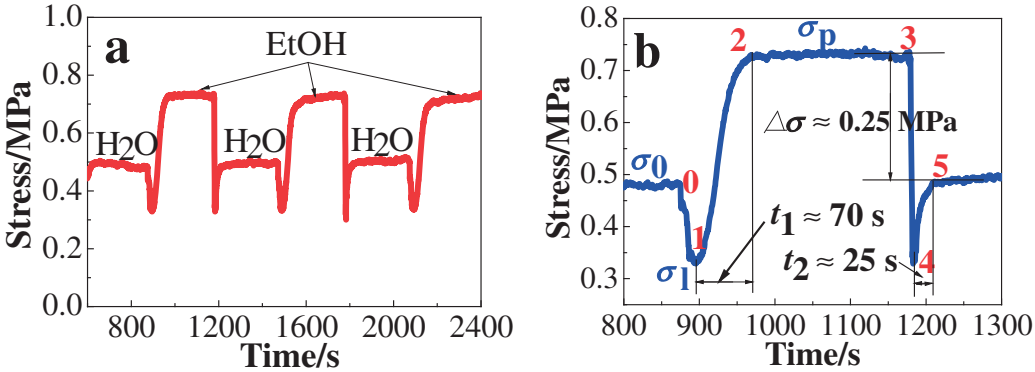

Figure 5. (a) Response in the isometric stress of the UTDN gels periodically triggered by EtOH and water; (b) magnification of the response cycle located at 800–1300 s presented in (a). Thickness of the UTDN gels used here was about 100 mm. The isometric contraction was performed at a tensile prestrain of 100%. Reproduced with permission from Ref. 71.

gels are transferred from water to EtOH, the stress first decreases from the initial value σ_0 in water to a valley σ_1, and then increases rapidly to a plateau (σ_p) that is higher than the initial value σ_0. Setting here $\sigma_0 = 0.48$ MPa as the base line, the contractile stress, $\Delta\sigma = \sigma_p - \sigma_0$, can reach $\approx$0.25 MPa. This value is comparable to $\approx$0.1 MPa of the real muscle in response to Ca^{2+} signal and $\approx$0.2 MPa of electrostatic silicone rubber triggered by strong electric field (144 V mm^{-1}).[67,72] Through changing the solvent component, we can continuously adjust $\Delta\sigma$ over a wide range. For example, the UTDN gels in 20 wt % water/80 wt % EtOH mixture only give $\Delta\sigma$ of about -0.12 MPa. This adjustability in $\Delta\sigma$ stems from the solvent-induced changes in the length and elastic modulus of the UTDN gels.

Furthermore, the response of UTDN gels to solvent-stimulus is very fast and well reversible. As shown in Figure 5b, clearly, two peak-like transitions $0 \rightarrow 1 \rightarrow 2$ and $3 \rightarrow 4 \rightarrow 5$, which indicate the fast response of the gels to the solvents, are observed. The sharp drop of σ_0 to σ_1 in $0 \rightarrow 1$ is attributed to the rapid softening process of the UTDN gels due to the presence of residual water. The process $1 \rightarrow 2$ corresponds to the hardening of the gels in response to the solvent change from the EtOH–water mixture to pure EtOH. With the characteristic contraction time of $t_{1\rightarrow2} = 14.8$ s, this process is mainly controlled by the diffusion of water molecules outward from the gel. Following $1 \rightarrow 2$, $\Delta\sigma$ reaches its maximum at the time scale of $t_1 = 50$–80 s and keeps almost constant until re-relaxed in water. The fast responses $3 \rightarrow 4$ and $4 \rightarrow 5$ are the fast resoftening of the contracted UTDN gels from EtOH to the transient EtOH–water mixture and the relative rehardening to the pure water, respectively. In $4 \rightarrow 5$, the fast drop of $\Delta\sigma$ from about 0.25 MPa to zero can be completed within $t_2 = 20$–30 s. The difference between t_1 and t_2 suggests a different hindrance for the diffusion of water in the gels.

According to these results, we can conclude that the UTDN gels developed based on DN principle possess both high mechanical strength and fast stimuli-responsive that can effectively serve as artificial muscles. In addition, the technique of synthesizing gel films with good toughness should expand the applications of DN gels as water filter membranes, contact lenses, wound dressings, etc.

4. Bonding between DN Gel and Porous Substrate

Owing to the excellent mechanical properties, low friction resistance, and good biocompatibility, DN gels possesses promising prospective in the application of these materials as tough artificial tissues such as artificial cartilage. At present most artificial joints, such as hip joints and knee joints, are made from hard, dry materials such as ceramics, ultrahigh molecular weight polyethylene, and metals.[73–75] These solid materials result in artificial joints with high friction, poor dispersion of loads, and poor absorption of impact energy, which are fundamental functions of real articular joints. Therefore, mechanically tough DN gels with a low sliding friction resistance are proposed to be the ideal material to make artificial cartilage and meniscus tissues. To realize these applications, however, one substantial obstacle to be resolved is how to form a strong bond between the soft, wet gel and the hard, dry solid, similar to the junction between ligament and bone.[76]

We have solved this problem by engineering a strong interface between a DN gel and a porous solid by anchoring the DN gel in the porous substrate, taking advantage of the DN principle.[77] This breakthrough starts from the invention of the strong bonding between two pieces of PAMPS gel sheets by polymerizing the second network PAAm inside both of the PAMPS gels and their interface, as shown in Figure 6a.[78] At first, the two pieces of the first network PAMPS gel sheets are prepared. Then, the prepared PAMPS gel sheets are dipped in the aqueous solution of the AAm monomer of the second network gels. After the gel sheets reach their equilibrium state in the aqueous solution, the two gel sheets are contacted and the second network PAAm gel is polymerized by UV irradiation. Thus, a united DN gel is obtained. Figure 6b shows this united DN gel during a tearing test.

The strength of the united bonding strongly depends on the preparation conditions. We should apply certain compressive stress on the contacting sheets of PAMPS during second polymerization to ensure the PAAm forms a continuously connected network at the interface. The crosslinker density in the second polymerization significantly affects the peeling energy which is defined as the energy to create a unit fractured surface between the two bonded gel sheets, as shown in

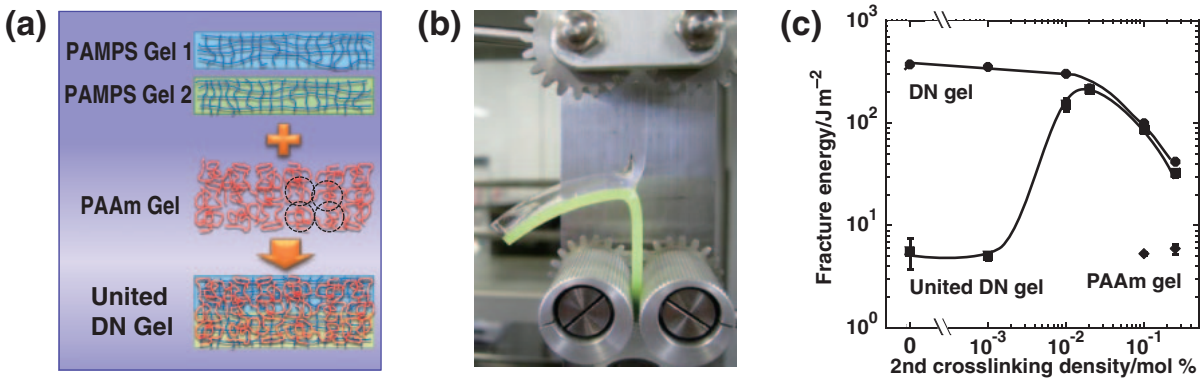

Figure 6. Robust bonding between hydrogels. (a) Schematic illustration of the formation of the DN structure between a pair of PAMPS gel sheets by synthesizing PAAm gel inside both the PAMPS gel sheets and the interface. The dashed circles in the PAAm polymer indicate the characteristic expanding length of PAAm polymer chain. (b) Photograph of the united hydrogel sheets prepared by applying the DN structure. The lower gel sheet was colored by yellowish green pigment for the eye. (c) Peeling fracture energy G (one half of the conventionally defined peeling energy T) of united DN gel in comparison with the fracture energy of the normal DN gels, as functions of the crosslinking density of the second network. The united DN gel was prepared with a negligible normal compression. Reproduced with permission from Ref. 78.

Figure 6c. When no or little (0.001 mol %) crosslinker is used, the peeling energy is very small, similar to a bulk single network ($\approx$6 J m^{-2}).[50] However, when the second crosslinker density increased to 0.01 mol %, the peeling energy steeply increased to a value as large as the fracture energy of the normal DN gels ($\approx$600 J m^{-2}). It should be noted that in this condition it is hard to recognize whether the fracture tip runs along the bonded surface or not. This implies that the peeling energy of the bonding interface of the united DN gels become comparable to the fracture energy of the bulk of the normal DN gels. After the peeling energy reaches the maximum value, it decreases as the second crosslinker concentration increases, which is similar to the decreasing tendency of the normal DN gels. As far as we know, such a strong bonding between hydrogels had not been achieved before.

The different effects of crosslinker concentration, C_{MBAA}, on the fracture energy between conventional DN gels and united DN gels come from the different apparent C_{MBAA}. Quite recently, we have elucidated that in the first PAMPS network gels a small amount of residual double bond (0.06 mol % in usual PAMPS gels) remains and reacts with AAm to form the chemical crosslinking between the first PAMPS network and the second PAAm network during the second polymerization.[49] The interaction between the PAMPS and PAAm networks in the DN structure is crucial for the efficient breaking process of the PAMPS gels. In the synthesis of second PAAm network in united DN gels, the interface has no residual double bond. This is why we obtain toughness in the conventional toughest DN gel when no additional crosslinker is added for the polymerization of the second PAAm network but $C_{MBAA} \approx 10^{-2}$ mol% for untied DN gels.

The effective enhancement of the adhesion between hydrogels is previously achieved by a sensible way of polymer interdiffusion, i.e., by the interpenetration of linear polymer chain into both the hydrogels.[79–81] Our approach is, however, conceptually advanced because the anomalous enhancement of the peeling energy is achieved by applying the DN-structure to the interface between hydrogels.

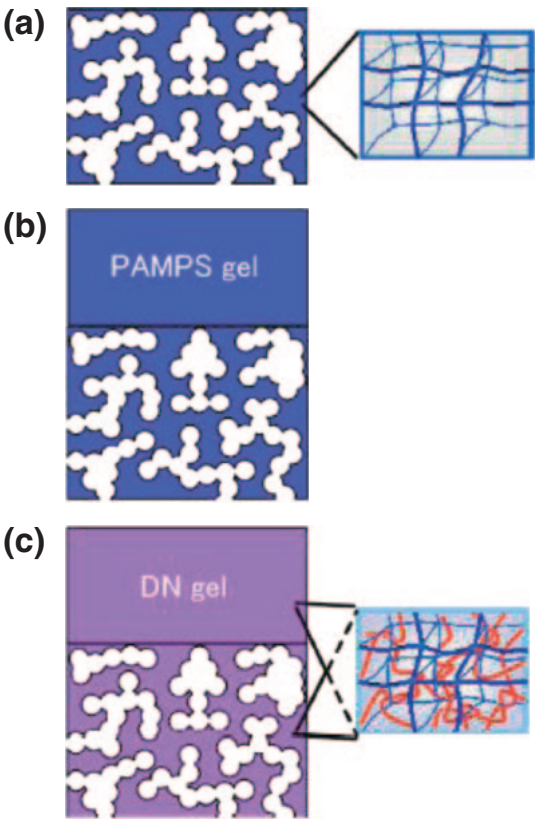

Figure 7. Schematic illustration of bonding (DN) gel to porous solid by anchoring the gel via DN structure formation. Reproduced with permission from Ref. 77.

This bonding technique is also applied to form united and tough interface between hydrogel and solid porous substrate such as glass plate.[77] Figure 7 illustrates the procedure for formation of an anchoring interface between a piece of tough DN gel sheet and a glass substrate with pore size of several micrometers. First, a PAMPS gel as the first network is

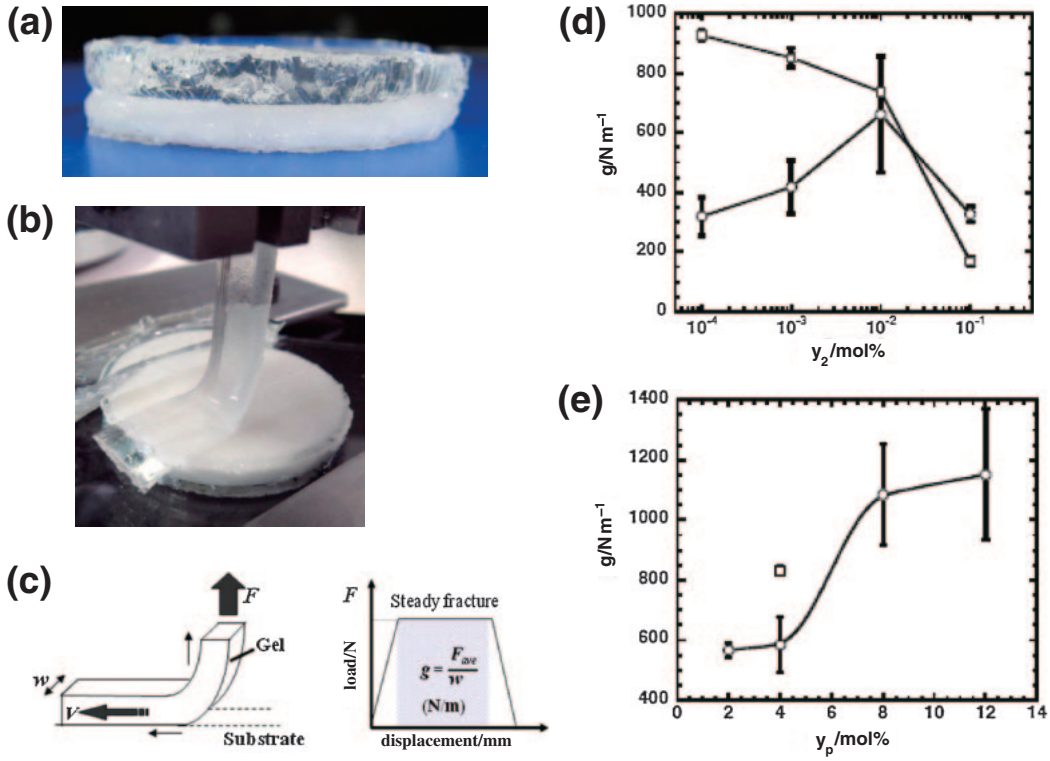

Figure 8. (a, b) Photographs of the DN gel–porous glass substrate interface (a) and the peeling measurements of the bonding strength to detach the gel from the solid (b). The bottom white part is the porous glass substrate. (c) Schematic of the peeling test conducted on the gel–solid substrate interface. Calculation of the peeling force per unit length, g. (d, e) Dependence of g on the crosslinker concentration in the second network, y_2 (d) and the crosslinker concentration of the first network in the porous substrates, y_p (e). (○) g of the interface between the DN gels and the glass substrate. (□) g of the bulk DN gel. Reproduced with permission from Ref. 77.

synthesized in the voids of the porous glass substrate (Figure 7a). Then the porous glass substrate containing the PAMPS gel is immersed in a pregel solution containing AAm. Subsequently, the porous solid is brought into contact with the PAMPS gel sheet that has been soaked in AAm solution (Figure 7b). After the second polymerization, a PAAm gel is simultaneously synthesized in both the porous glass and in the PAMPS sheet (Figure 7c). Using this method a continuous network of PAAm is formed in the porous glass substrate and the PAMPS gel sheet. This method affords a DN structure in both the porous solid and in the gel sheet. The DN gel sheet is firmly anchored to the porous solid due to osmotic swelling pressure.

A side view of the DN gel–solid interface is shown in Figure 8a. The transparent upper portion is the DN gel, while the white lower portion is the porous glass substrate. To measure the peeling strength of the interface, the bonding DN gel is cut into 5 mm wide strips from the disk-shaped porous glass substrate. A notch is made by cutting the specimen at the DN gel–solid interface. The porous solid is glued onto the substrate holder of a compressive tensile tester and one arm of the trouser-shaped gel is clamped to the tester (Figure 8b). The bonding strength is characterized by the peeling force per unit length, g, to detach the gel from the solid, as schemed in Figure 8c.

Figure 8d shows the effect of the crosslinker concentration used in synthesis of PAAm on the peeling force per unit length, g, when the composition of PAMPS gel is identical in both the porous substrate and the PAMPS gel sheet. The second step polymerization is performed using a constant amount of monomer and initiator while changing the amount of crosslinker. The g of the gel–solid interface increases when the crosslinker concentration in PAAm is increased to 10^{-2} mol%. If the crosslinker concentration in PAAm exceeds 10^{-2} mol%, both g at the interface and g of the bulk DN gel quickly decrease. This result is in agreement with that of united DN gels (the bonding two pieces of gels, Figure 6c).[49,78] By carefully investigating the surface of the porous substrate containing the PAMPS gel we found that the surface of the PAMPS gels is very rough, probably owing to the restricted free swelling of PAMPS in the aqueous AAm solution. This rough and modulated surface prevents complete contact between the PAMPS gel in the solid porous substrate and the upper flat PAMPS gel sheet. To reduce the swelling of the PAMPS gel in the porous substrate, we can increase the crosslinker concentration in the PAMPS gel network in the pores of the glass substrate, while keeping the crosslinker concentration in the PAMPS gel sheet constant, 4 mol %. As shown in Figure 8e, g increases with increasing crosslinker concentration of the PAMPS gel in the pores. At crosslinker concentrations of 8 and 12 mol % g of the gel–substrate interface exceeds 1000 N m^{-1}, which is almost twice the value of g observed when the crosslinker concentration is 2 and 4 mol %.

For a nonporous substrate, particularly one with a rough surface, the gel–substrate interface is too weak for the strength to be measured by the peeling test. This indicates that an increase in the extent of interfacial contact is not crucial to increasing the bond strength. Rather, the anchoring effect, i.e., confinement of the DN gel in the micropores, is responsible for the high bond strength. Investigation of the fractured surfaces of the gel–solid interfaces reveals that failure occurs not because of the detachment of gel from the micropores but because of the rupture of gel at the interface. This indicates that the anchoring strength is higher than the interface strength. We believe that the methodology to tightly bond gels to solid by anchoring the gel to porous substrate will substantially broaden the applications of tough gels. For example, artificial cartilage made of DN gels bonded with porous hydroxyapatite could be used to manufacture artificial joints.

5. Free-Shaping of DN Gels

Another difficulty of the conventional DN gels in the application to artificial tissues is lack of formability. For example, it is required for an artificial cartilage to form any specific complex shape dependent on the body of each patient. However, conventional DN gels can be formed only in limited shapes, such as a sheet or a disc. The shapes of DN gels are determined by the first network PAMPS gels acting as a "skeleton" due to the two-step polymerization. Although PAMPS gels themselves can be formed in any shapes by using molds, it is very difficult to eject convoluted PAMPS gels without breaking them due to their extremely poor mechanical properties, such as 0.08 MPa of tensile fracture stress, 0.36 of tensile fracture strain and $0.8\,J\,m^{-2}$ of fracture energy. Incidentally, PAMPS gels or DN gels also cannot be cut or scraped into the desired shape after the synthesis. We have solved this problem in two different ways by applying a "double network" structure.

5.1 Poly(vinyl alcohol) Gel as Internal Mold to Free-Shaping DN Gels. As previously mentioned, the shape of DN gels is determined by the first network. Based on this fact, it is imagined that if PAMPS gels are synthesized in another kind of hydrogel which is strong enough to eject from molds, the shape of them can be modified easily. We call these shape-deciding hydrogels "internal molds," as the opposite concept of conventional "external" molds.[82] The physically crosslinked poly(vinyl alcohol) gels (PVA gels) are used as internal molds because they are so flexible and relatively strong that they can form many complicated shapes.[83]

The free-shaped tough gels are synthesized as follows.[82] First, the PVA gels with complex shapes are synthesized. Second, the PAMPS network is polymerized in the PVA gels. Third, the PAAm network is synthesized in the presence of the PVA/PAMPS double-network gels (PVA/PAMPS gels) and finally the free-shaped PVA/PAMPS/PAAm triple-network gels (PVA-DN gels) are obtained. These PVA-DN gels show similar mechanical properties to the conventional DN gels. By this method, any complicated shapes can be formed, such as the bird, the fish, and the Chinese knot shape depending on the shape of the PVA gels used as the internal mold (Figure 9).

Figure 10 shows pictures of a sphere-shaped PVA-DN gel hit by a golf club, recorded by a high-speed camera. In spite of the strong impact and the large deformation, the PVA-DN gel recovers to its original shape without breaking. In contrast, the PVA/PAMPS gel is catastrophically broken by the impact. To quantitatively characterize the toughness of the gels, we measured the fracture energy, G, of the PVA-DN, conventional DN, and PVA/PAAm DN gels (Figure 11a). G of the PVA-DN gels was anomalously high and similar to that of the conventional DN gels. To clarify the effect of the PVA chains on the toughness of the PVA-DN gels, we investigated the effect of PVA network by measuring G of the PVA-DN gels before and after heating. Physical PVA gels are crosslinked by the formation of hydrogen bonds that are easily destroyed by heating. Therefore, the effect of the PVA network on the mechanical properties of PVA-DN gels can be removed by heating the samples. The DN gels, the PVA-DN gels, and the PVA gel are immersed in hot water at 70 °C for 8 h. The G of the conventional DN gels and the PVA-DN gels do not change by this operation. This result implies that the PVA network of PVA-DN gels has no effect on the mechanical strength of DN gels. The PVA network works only as an "internal mold."

Figure 11b shows the tensile stress–strain curves of the DN gels. The tensile fracture stress of the PVA-DN gels is less than that of DN gels, however, the fracture strain of those gels was similar to each other. This phenomenon might be caused by a lower PAMPS concentration in the PVA-DN or PVA/PAMPS gels than conventional PAMPS gels and DN gels. As the PVA gels contained 10 wt % polymer, concentration of AMPS in the

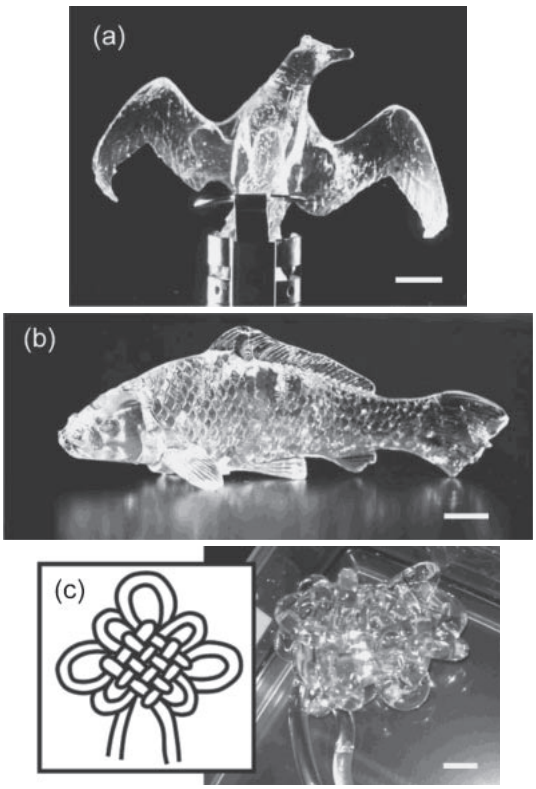

Figure 9. Images of the PVA-DN gels with the shape of the bird (a), the fish (b), and the Chinese knot (c). Conventional PAMPS gels and DN gels cannot form such complicated shapes. Scale bars: 1 cm. Reproduced with permission from Ref. 82.

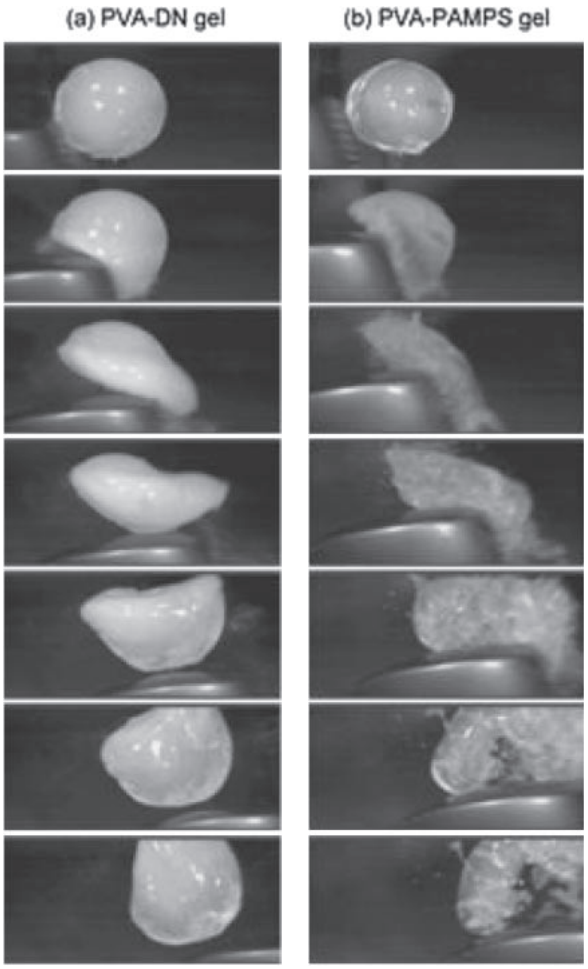

Figure 10. High-speed camera images of the spherical PVA-DN gel (a) and PVA/PAMPS gel (b) being hit by a golf club. The time interval between each picture is 3/4000 s. Reproduced with permission from Ref. 82.

PVA/PAMPS gels cannot reach 1 M in spite of the gel immersion in 1 M AMPS solution.

Although PVA/PAAm DN gels also show formability, their fracture energy G is much lower than that of the other DN gels. In addition, no yielding and necking appear during the tensile test. These results indicate that the existence of PAMPS network is crucial for the toughing of PVA-DN gels (the coupling of two soft polymers, PVA and PAAm, cannot lead to high mechanical strength). As we mentioned before, the brittle PAMPS network, serving as sacrificial bonds and breaking into small clusters during the large deformation, is essential for the toughing of PVA-DN gels.

The Young's modulus of the PVA/PAMPS gels, the conventional PAMPS gels, and the PVA gel in swollen state is shown in Figure 11c. The conventional PAMPS gels show the highest modulus (≈0.25 MPa). The PVA/PAMPS gels also have high modulus (≈0.15 MPa), although the values are less than those of PAMPS gels. It suggests that despite the presence of the PVA network, the modulus of the swollen PVA/PAMPS gels is mainly dominated by rigid PAMPS networks due to the full stretching of polyelectrolyte chains. This rigidness leads to the toughening of DN gels; thus, both the PVA-DN gels and the

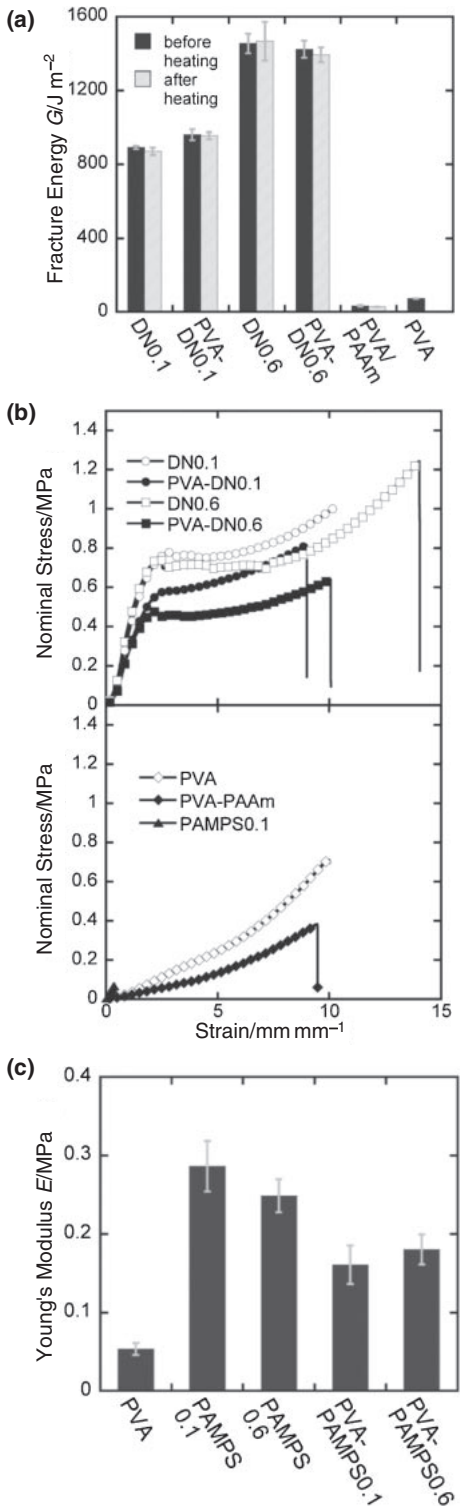

Figure 11. (a) The fracture energy, G, of the PVA-DN gels, the conventional DN gels, the PVA/PAAm gel, and the PVA gel. The filled and mesh bars represent G of the DN gels before and after heating, respectively. The tearing velocity was 250 mm min^{-1}. (b) The tensile stress–strain curves of the gels. The PVA/PAMPS gels are too weak to be measured. The tensile velocity was 100 mm min^{-1}. (c) Young's modulus of the PVA gel, the swollen PAMPS gels, and the swollen PVA/PAMPS gels. Reproduced with permission from Ref. 82.

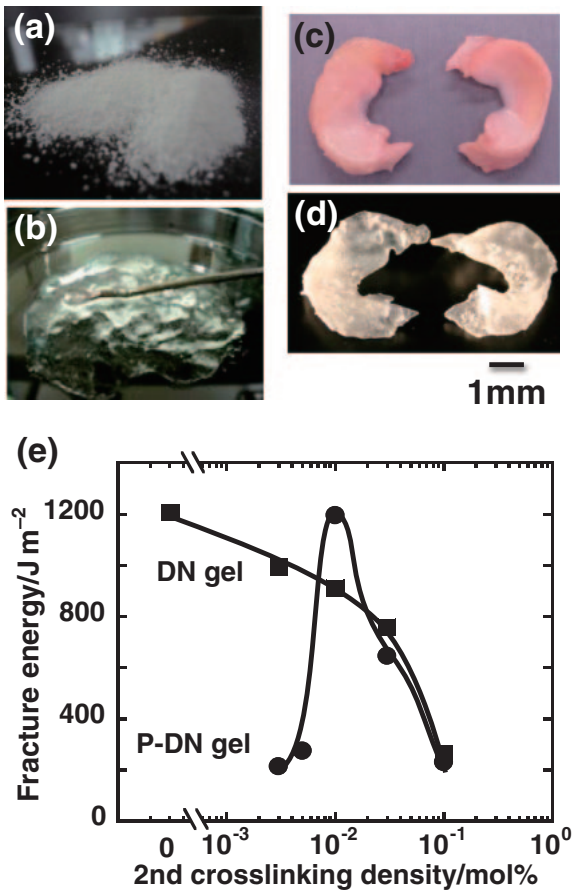

Figure 12. Particle DN (P-DN) gels with free shapes and toughness synthesized from PAMPS particles. (a) PAMPS gel particles (powders) in dried state. (b) Swollen PAMPS particles in AAm aqueous solution before gelation. (c, d) A pair of rabbit meniscus (c) and artificial meniscus made from P-DN gels (d). (e) Fracture energy of free-shape P-DN gels and normal DN gels, as functions of the crosslinking density of the second network PAAm. Reproduced with permission from Ref. 78.

DN gels possess toughness.[84] In contrast, the modulus of the swollen PVA gel is quite low (≈0.05 MPa), even though its polymer concentration is much higher than that of the swollen PAMPS gels. Therefore, the PVA/PAAm DN gels do not show toughness.

Based on the above results, we obtain the formability of DN gels by introducing the flexibility of as-prepared first network gels, e.g., using PVA/PAMPS gels as the first network. The extremely high mechanical strength is derived from the rigidity of swollen PAMPS networks. They are flexible (and soft) enough to form any shape in as-prepared PVA single network state. After the synthesis of PAMPS network inside the PVA gel and the swelling process, they become rigid (and brittle), which enables toughening (PVA-)DN gels. This is the reason why PVA/PAMPS/PAAm (PVA-DN) gels have both formability and toughness.

5.2 Particle-DN Gels with Free Shapes. Another method to develop free-shaped tough gels is the synthesis of DN gels from PAMPS particles.[78] On the basis of the experiments about the united bonding by virtue of the DN structure, we can expect that many small pieces of PAMPS gels can be bonded together by introducing the second PAAm network to form a united tough bulk DN gel with complicated shapes. We grind PAMPS bulk gels into particles with several tens of micrometers in diameter and then dry them (Figure 12a). The obtained dried PAMPS particles are then soaked in AAm solution to form paste-like solution (Figure 12b). By polymerizing the AAm of the paste-like solution, DN gels from the PAMPS particles, named "P-DN gels," are formed. As presented in Figures 12c and 12d, by using this PAMPS particle precursor method, we can synthesize P-DN gels with the same complicated shape of the rabbit meniscus by using molds with complex shape. This method also makes it possible to synthesize the P-DN gels containing versatile particles.[85] The P-DN gels have the advantages of easy and quick preparation and free-shape forming. While it is difficult to synthesize a conventional DN gel with a desirable complex shape due to the brittleness and size change under swelling of the PAMPS gels, it is easy to handle the paste-like PAMPS particle solutions in molds of various shapes.

The mechanical strength of P-DN gels strongly depends on the crosslinker concentration of the PAAm network. Figure 12e shows the fracture energies of P-DN gels and conventional DN-gels, as functions of the crosslinker concentration. We found that the fracture energy of P-DN gels rapidly increases with the increase in the amount of crosslinker used for the polymerization of the PAAm network, and reaches a maximum at 0.01 mol % of the crosslinker. Further increase in crosslinker concentration results in the quick decrease in the fracture energy of P-DN gels. This result coincides well with the effect of crosslinker concentration on the peeling energy of the united DN gel and the peeling force per width of gel–solid interface,[49,77,78] indicating that these systems share the same toughening mechanism.

The two techniques enable the synthesis of tough DN gels with free-shape and therefore to be applied in biological and industrial fields, such as artificial cartilages adopted into individual patients, artificial blood-vessels with complicated shapes, and gel machines based on chemomechanical systems.

6. Mechanical Strength of Anisotropic Hydrogels Enhanced by DN Structure

Most soft biotissues, natural hydrogels such as ligaments, possess both mechanical strength and well-ordered structure that play a significant role in executing the functions of living organisms.[86–88] There have been many efforts toward developing macroscopically ordered hydrogels with additional functionalities by molecular self-assembly of biopolymer, amphiphile, block-copolymer, and liquid crystal molecules.[89–92] The developed structured gels with single network show good optical and electric properties, and smart response to environmental stimuli. However, they usually lack mechanical strength that greatly limits their applications in tissue engineering, soft actuators, and mechanical–optical sensors. The mechanical properties can be significantly improved by applying the DN structure. To show the capacity of this method, we simply introduce two kinds of enhanced anisotropic hydrogels, in which biomacromolecular fibers or physically crosslinked liquid crystalline polymers serve as the first network.

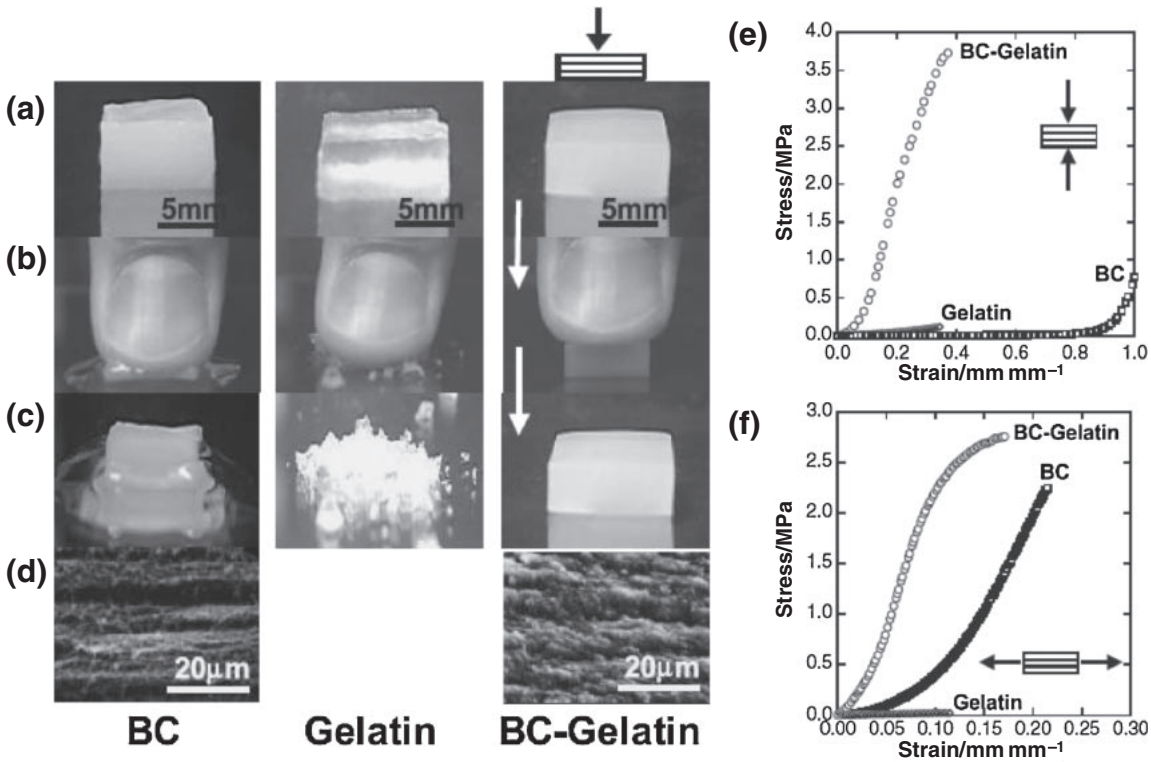

Figure 13. (a–c) Pictures of the BC, gelatin, and BC–gelatin DN gels before (a), during (b), and after compression. (d) Scanning electron microscope (SEM) images of the stratified structure of the BC and BC–gelatin DN gels. (e, f) Compressive (e) and tensile (f) stress–stain curves of gelatin gel, BC gel, and BC–gelatin DN gel. The compression and tensile were performed perpendicular and parallel to the stratified direction of the BC and BC–gelatin DN gels. Reproduced with permission from Ref. 95.

6.1 Bacterial Cellulose Double Network Hydrogels. Bacterial cellulose (BC) is a form of extracellular cellulose produced by bacteria of the genus *Acetobacter* such as *Acetobacter xylinum* and consists of a hydrophilic ultrafine fibril network stack in a stratified structure.[93,94] BC gels have high tensile strength along the fibril layer direction, but low compressive modulus properties perpendicular to the stratified direction. Water in a BC gel is easily squeezed out after slight compression, such as finger pressure, after which the swelling does not recover due to hydrogen-bond formation between cellulose fibrils (Figures 13a–13c).[95] We select gelatin as the second network to form DN structure with the first BC gel and therefore to improve the mechanical properties of BC gel. It is because gelatin is a polypeptide derived from an extracellular matrix collagen, and gelatin gel can retain water and recovers from repeated compression.

The synthesis process is as follows. The purified BC gel is immersed in an aqueous solution of gelatin at 50 °C for a week and then immersed in an aqueous solution of *N*-(3-dimethylaminopropyl)-*N*′-ethylcarbodiimide hydrochloride (EDC) for 4 days at room temperature to allow the occurrence of chemical crosslinking. The stratified structure of BC is well-maintained in the BC/gelatin DN gel, as shown in the scanning electron microscopy (SEM) image of Figure 13d. The chemically crosslinked gelatin gel is isotropic and mechanically brittle; it is easily broken into many fragments simply by pressing with a finger. In contrast, the BC/gelatin DN gel can hold water even under pressures as high as 3.7 MPa and completely recovers its original shape even after repeated compression in the direction perpendicular to the stratified structure of the developed DN gel.

Figure 13e and Figure 13f show the typical compression and tensile stress–strain curves of BC, gelatin, and their composite BC/gelatin DN gels.[95] The compression and tension are applied in the direction perpendicular and parallel, respectively, to the stratified structure of the BC and BC/gelatin gels. The BC/gelatin DN gel shows a quite different compression stress–strain profile compared with individual BC and gelatin gels. The compressive elastic modulus of the composite gel is ≈1.7 MPa, which is ≈240 times that of the gelatin gel (0.16 MPa). The compression fracture stress of the composite DN gel reaches 3.7 MPa, which is ≈30 times higher than that of gelatin (0.12 MPa). According to the tensile test, BC/gelatin DN gel can sustain ≈3 MPa and has a tensile elastic modulus of 23 MPa, which is 112 times larger than that of gelatin gel. Furthermore, a cyclic compressive test demonstrates that BC gel does not retain its original stress–strain profile, whereas the BC/gelatin DN gel recovers well from a second compression deformation up to 30% strain. Thus, the DN structure leads to a substantial improvement of the mechanical properties of BC gels. Similar improvement in the mechanical strength is also obtained by combinations of BC with polysaccharides, such as sodium alginate and gellan gum.

We can further improve the mechanical strength of BC gel by introducing ductile PAAm as the second network.[96] As shown in Figure 14, the compressive and tensile fracture stress of BC/PAAm DN gels reaches ≈6 MPa and 40 MPa,

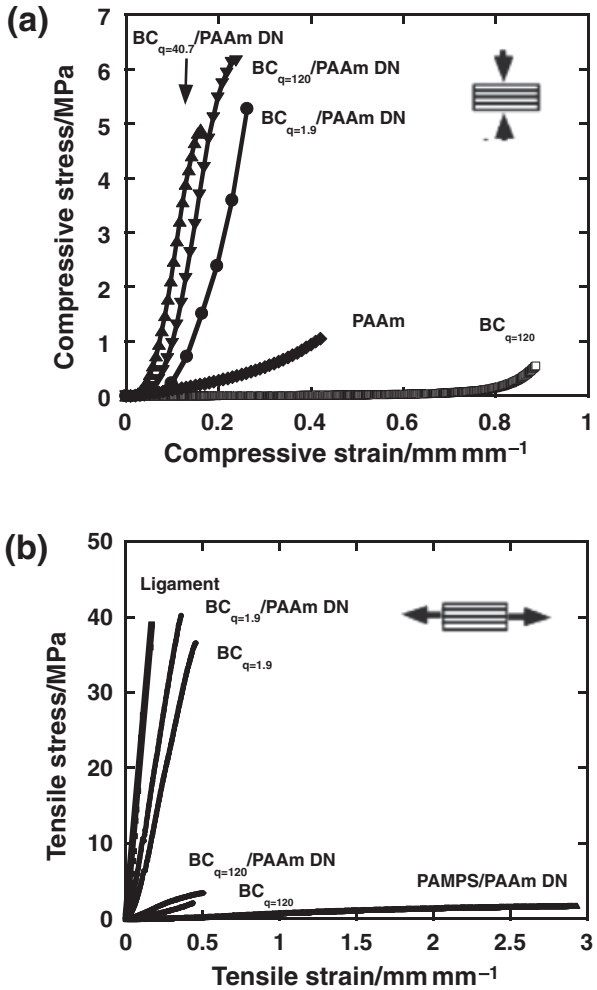

Figure 14. Compressive (a) and tensile (b) stress–stain curves of BC, PAAm, and BC/PAAm DN gels with controlled BC water content. The swelling degree, q, of BC gels, defined as the ratio of the weight of the as-prepared swollen sample to that of the dry sample, was controlled by compressing the as-prepared BC gels appropriately. The tensile stress–strain curve of biological ligament is shown in (b) for a reference. Reproduced with permission from Ref. 96.

respectively, which are comparable to that the biological ligaments.

6.2 Anisotropic Liquid Crystalline DN Gels. Liquid crystalline hydrogels (LC gels) are recognized as a typical functional soft material toward soft robotics, which exhibit good optical properties, anisotropic conductivities, and fast shrinking, and fast response to stimuli.[89–92] However, these single network LC gels usually have poor mechanical properties that limit their application in developing chemomechanical systems such as stress/strain sensors. We can create a DN structure in the general LC gels to overcome the weakness of poor mechanical strength.

A physically crosslinked, macroscopically anisotropic hydrogel of poly(2,2′-disulfo-4,4′-benzidine terephthalamide) (PBDT) is used as the first network. Physical PBDT gel is synthesized by using a dialysis method initially developed by Dobashi and co-workers.[97–100] Anisotropic hydrogel was obtained by the simple diffusion of a multivalent salt $CaCl_2$ into the semirigid polyanion PBDT solution, where Ca^{2+} behaves as a physical crosslinker.[101,102] Then, physical PBDT gel is immersed in a precursor solution of AAm. After a subsequent photopolymerization, PBDT/PAAm anisotropic DN gel (A-DN gel) is obtained by the synthesis of second loosely crosslinked PAAm network in the first physical PBDT gel (Figure 15a).[101,103]

Figure 15b presents the image of the PBDT/Ca^{2+} physical gel observed under polarizing optical microscope with insertion of 530 nm tint plate. From the birefringent colors we can distinguish the molecular orientation of PBDT in the gel.[102–106] In the outer region of the gel, PBDTs align perpendicular to the diffusion direction of Ca^{2+}; this structure is also confirmed by small-angle X-ray scattering measurement.[102,105,106] Both the oriented structure and birefringence can be fully maintained after introducing the second network. The incorporation of the condensed, flexible PAAm chains greatly improves the mechanical properties of the physical PBDT gel without disturbing the staggered bundle structure of PBDT. The samples for tensile test are cut from the outer region of the A-DN gel in two directions, parallel and vertical to the alignment of PBDT molecules (Figure 15c), noted as A-DN parallel and A-DN vertical.

The physical PBDT gels are very brittle. The tensile fracture strain and stress are less than 0.8 and 0.25 MPa (Figure 16a). In contrast, A-DN gels possess robust mechanical properties, especially excellent extensibility (Figure 16b). The A-DN parallel sample exhibits a yield point at 25 kPa. On the other hand, the A-DN vertical sample, as well as the PAAm gel containing PBDT, does not have the yielding point but shows a similar curve as the PAAm gel. The existence of yielding point and relatively high elastic modulus in A-DN parallel sample is in agreement with the preferential alignment of PBDTs perpendicular to the diffusion direction.

The robust mechanical properties of A-DN gels enable the application of these gels as stress-optical sensor, because the stress/strain will lead to molecular orientation along the tensile direction and therefore the birefringence change (Figure 17a).[102] In the A-DN gel, the birefringence change becomes more interesting since the two networks have different optical properties. PBDT is an optically positive LC polymer, whereas PAAm shows a negative birefringence after the elongation-induced molecular orientation.

The original A-DN vertical sample shows a negative sign birefringence before elongation at strain $\varepsilon = 0$, however, the birefringence reverses to positive after a slight elongation at $\varepsilon > 0.2$ (Figure 17b). This birefringence reversion is confirmed by the birefringent images observed under polarizing microscope. In terms of the birefringent colors, we found that PBDTs orient in northwest direction in image D and in southwest direction in image F of Figure 17c. That is to say, the slight elongation induces the molecular reorientation of PBDT and the reversion of birefringence. At the relatively small strain, the strain-induced molecular orientation and birefringence of PAAm chains is negligible (the PAAm gel just starts to show weak birefringence when $\varepsilon > 3$). We note that the image C in Figure 17c showed yellow birefringence is because of the

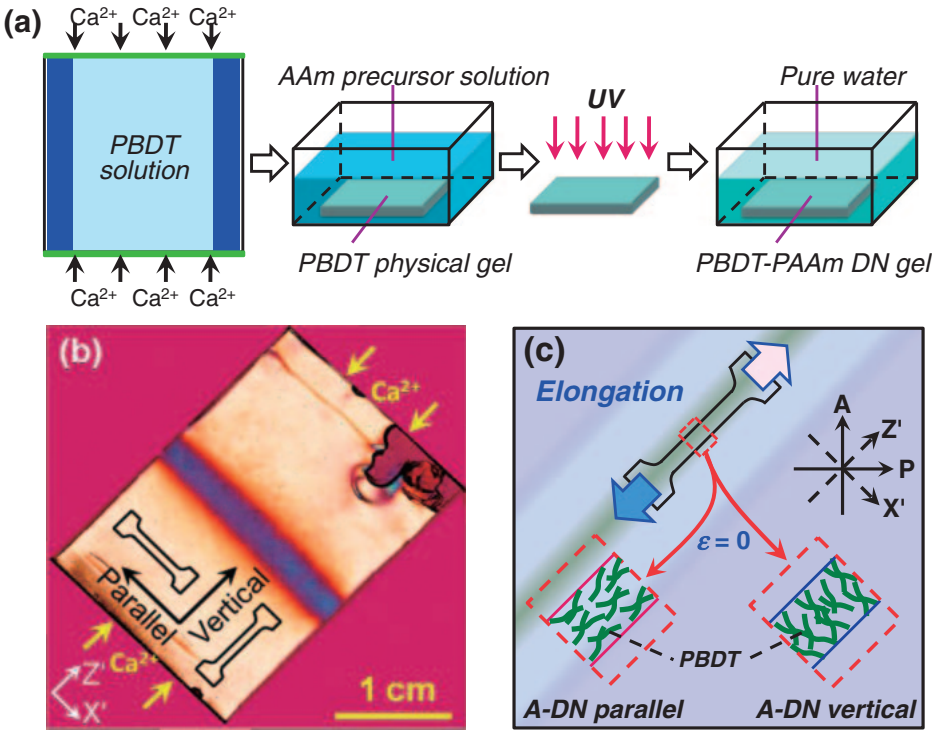

Figure 15. (a) Scheme for the synthesis of anisotropic double-network gel. The first network is a physically crosslinked LC gel synthesized by dialysis of PBDT solution in Ca^{2+} aqueous solution. (b) Images of synthesized 1 wt % gel observed under crossed polarizers with 530 nm tint plate. Arrows show the Ca^{2+} diffusion direction during the synthesis of the gel. (c) Illustration of the sample preparation for the tensile test. Parallel and vertical noted in (b) indicate that the sample and following elongation is parallel or perpendicular to the alignment of PBDT molecules, as shown in (c). In the illustration of (c), Ca^{2+} ions and PAAm chains are omitted for simplicity. A: analyzer; P: polarizer; X′: fast axis of the tint plate; Z′: slow axis of the tint plate. Reproduced with permission from Ref. 103.

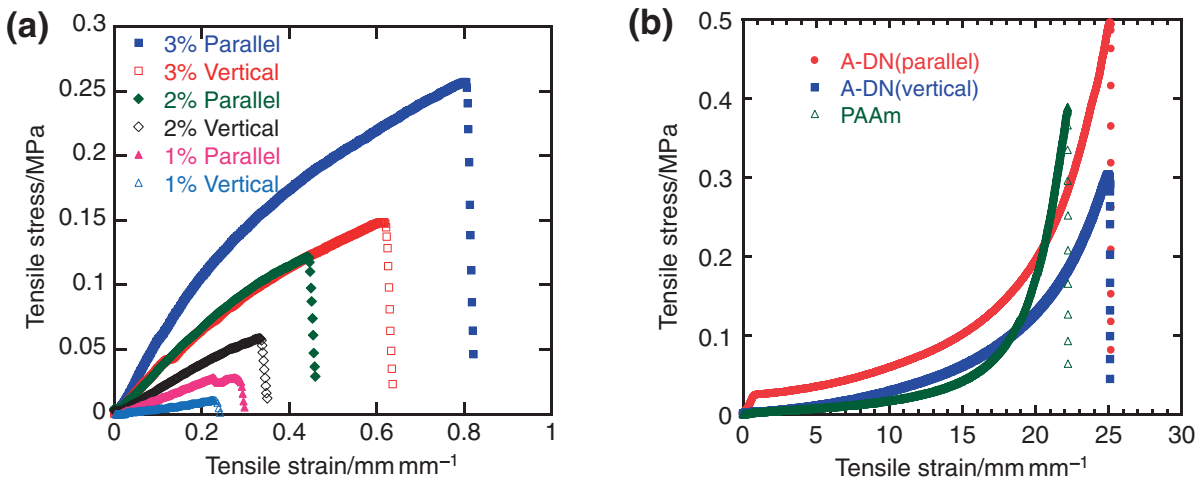

Figure 16. Tensile stress–strain curves of the physical PBDT gels with different PBDT concentrations (a) and A-DN gel (b) in parallel and vertical direction. Tensile stress–strain of PAAm gel is also shown in (b). (a) and (b) are reproduced with permission from Refs. 102 and 103, respectively.

birefringence shifting into the second-order color rather than the birefringence reversion.

The essential origin of the apparent alignment reversion of PBDT in A-DN vertical sample comes from the staggered PBDT and its fibrous bundle with slightly preferential alignment. The preferential alignment of PBDT and its fibrous bundle is vertical to the elongation direction and easily surpassed by the alignment parallel to the elongation. On the other hand, the A-DN parallel sample with PBDT alignment parallel to the elongation has no alignment reversion of PBDT, and therefore does not show the birefringence reversion. An overall picture for the change of birefringence and molecular alignment in A-DN gel with the applied stress/strain is proposed in Figure 17d.

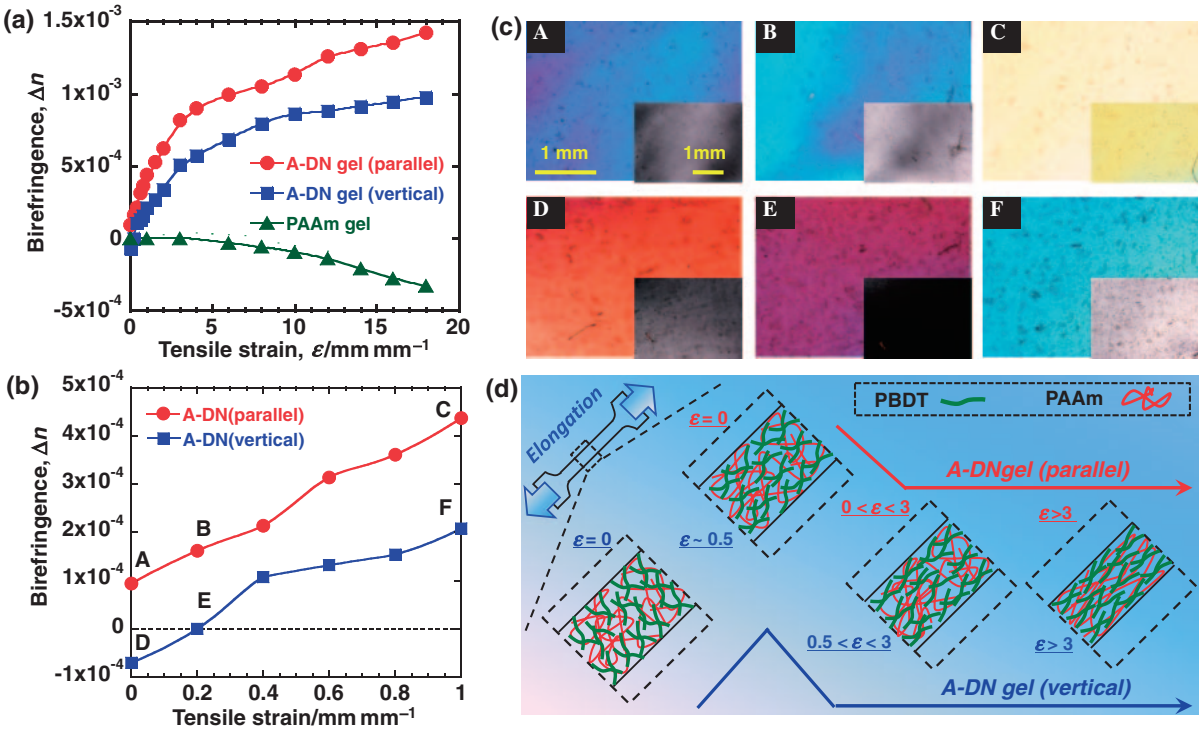

Figure 17. (a) Birefringence change of A-DN gel elongated along the direction in parallel and vertical to PBDT alignment, PBDT-containing PAAm gel, and PAAm gel under various strains. (b) Enlarged plot to show the birefringence change of parallel and vertical A-DN gels with small strains ($\varepsilon < 1$). (c) Optical micrographs of the A-DN gels observed under crossed polarizers with 530 nm tint plate, Micrographs A–F correspond to points A–F in (b); the inserts are the images observed under crossed polarizers without tint plate. (d) Illustration of the orientation change of PBDT and PAAm molecules in A-DN gels during the elongation. Reproduced with permission from Ref. 103.

The above two examples demonstrate that creating a DN structure in single network structured hydrogels effectively improves their mechanical strength, and therefore substantially broaden the applications of these functional materials in artificial tissues and chemomechanical systems. Essentially, the mechanical properties of any single network hydrogel can be enhanced by coupling an appropriate second polymer based on the DN principle.

7. Concluding Remarks for Future Scope

Conventional DN gels, consisting of the double network structure with strong contrasting properties of the two networks, possess excellent mechanical properties although they include ≈90 wt % water. Following this DN principle, several new systems and techniques are developed to address the specific problems in the applications of hydrogels as tough artificial tissues, soft robotics, etc. Our research on ultrathin DN film, bonding DN gel to a solid substrate, free-shaped tough gels, and the enhancement of a given single network gel based on DN structure should substantially expand the application of DN gels in both medical and industrial fields.

We should point out that the DN gel has a negligible fatigue resistance, which will be a limitation in many practical applications. This limitation arises from the fact that the toughening is due to the irreversible failure of covalent bonds in the first network.[26,55,56,59] However, the DN gel concepts can, in principle, be applied to other self-healing types of materials,[107–110] if the covalent bonds are replaced by reversible bonds. The challenge is to obtain bonds that are both strong and reversible. Recently, we have developed anisotropic hydrogel that has membrane-like lamellar bilayer structure with unidirectional alignment.[111] This gel showed excellent toughness, self-recovery and fatigue resistance.[112] Another challenging direction is how to create tough gels suitable for three-dimensional cell culture. Recent studies show that DN gels have good biocompatibility and are a good scaffold for cell cultured on the surface. However, developing tough scaffolds for 3-dimensional cell culture is also necessary since it can mimic some cell growth in typical environments, such as the chondrocyte in biological cartilage. Furthermore, it should be good to implant the artificial tissues cultured with cells in body to help the repair and regeneration of living organs.

This research was financially supported by a Grant-in-Aid for Specially Promoted Research (No. 18002002) from the Ministry of Education, Culture, Sports, Science and Technology of Japan. The authors sincerely thank Prof. Y. Osada, Prof. H. Furukawa, Prof. Y. Tanaka, Prof. A. Kakugo, Dr. Y.-H. Na, Dr. S. M. Liang, Dr. T. Nakajima, and the graduate students in Laboratory of Soft and Wet Matter, Hokkaido University for their contributions to this work.

References

1 *Polymer Gels: Fundamentals and Biomedical Applications*, ed. by J. D. DeRossi, K. Kajiwara, Y. Osada, A. Y. Yamauchi, Plenum Press, New York, **1991**.

2 J. P. Gong, N. Hirota, A. Kakugo, T. Narita, Y. Osada, *J. Phys. Chem. B* **2000**, *104*, 9904.
3 T. Tanaka, E. Sato, Y. Hirokawa, S. Hirotsu, J. Peetermans, *Phys. Rev. Lett.* **1985**, *55*, 2455.
4 Y. Osada, H. Okuzaki, H. Hori, *Nature* **1992**, *355*, 242.
5 Y. Osada, J. P. Gong, *Adv. Mater.* **1998**, *10*, 827.
6 C.-C. Lin, A. T. Metters, *Adv. Drug Delivery Rev.* **2006**, *58*, 1379.
7 J. L. Drury, D. J. Mooney, *Biomaterials* **2003**, *24*, 4337.
8 R. Langer, D. A. Tirrell, *Nature* **2004**, *428*, 487.
9 M. P. Lutolf, J. A. Hubbell, *Nat. Biotechnol.* **2005**, *23*, 47.
10 P. Calvert, *Adv. Mater.* **2009**, *21*, 743.
11 N. K. Simha, C. S. Carlson, J. L. Lewis, *J. Mater. Sci.: Mater. Med.* **2004**, *15*, 631.
12 A. J. Kerin, M. R. Wisnom, M. A. Adams, *Proc. Inst. Mech. Eng., Part H* **1998**, *212*, 273.
13 C. W. McCutchen, *Lubrication of Joints, the Joints and Synovial Fluid*, Academic Press, New York, **1978**.
14 J. Zarzycki, *J. Non-Cryst. Solids* **1988**, *100*, 359.
15 Y. Tanaka, K. Fukao, Y. Miyamoto, *Eur. Phys. J. E: Soft Matter Biol. Phys.* **2000**, *3*, 395.
16 D. Bonn, H. Kellay, M. Prochnow, K. Ben-Djemiaa, J. Meunier, *Science* **1998**, *280*, 265.
17 G. J. Lake, A. G. Thomas, *Proc. R. Soc. London, Ser. A* **1967**, *300*, 108.
18 K. Stok, A. Oloyede, *Clin. Biomech. (Bristol, Avon)* **2007**, *22*, 725.
19 Y. Tanaka, J. P. Gong, Y. Osada, *Prog. Polym. Sci.* **2005**, *30*, 1.
20 J. A. Johnson, N. J. Turro, J. T. Koberstein, J. E. Mark, *Prog. Polym. Sci.* **2010**, *35*, 332.
21 Y. Okumura, K. Ito, *Adv. Mater.* **2001**, *13*, 485.
22 K. Ito, *Polym. J.* **2007**, *39*, 489.
23 K. Haraguchi, T. Takehisa, *Adv. Mater.* **2002**, *14*, 1120.
24 K. Haraguchi, *Polym. J.* **2011**, *43*, 223.
25 J. P. Gong, Y. Katsuyama, T. Kurokawa, Y. Osada, *Adv. Mater.* **2003**, *15*, 1155.
26 J. P. Gong, *Soft Matter* **2010**, *6*, 2583.
27 M. Malkoch, R. Vestberg, N. Gupta, L. Mespouille, P. Dubois, A. F. Mason, J. L. Hedrick, Q. Liao, C. W. Frank, K. Kingsbury, C. J. Hawker, *Chem. Commun.* **2006**, 2774.
28 K. Zhang, M. A. Lackey, J. Cui, G. N. Tew, *J. Am. Chem. Soc.* **2011**, *133*, 4140.
29 T. Sakai, T. Matsunaga, Y. Yamamoto, C. Ito, R. Yoshida, S. Suzuki, N. Sasaki, M. Shibayama, U-i Chung, *Macromolecules* **2008**, *41*, 5379.
30 S. H. Yoo, C. Cohen, C.-Y. Hui, *Polymer* **2006**, *47*, 6226.
31 S. S. Jang, W. A. Goddard, III, M. Y. S. Kalani, *J. Phys. Chem. B* **2007**, *111*, 1729.
32 D. Myung, N. Farooqui, D. Waters, S. Schaber, W. Koh, M. Carrasco, J. Noolandi, C. W. Frank, C. N. Ta, *Curr. Eye Res.* **2008**, *33*, 29.
33 L. Weng, A. Gouldstone, Y. Wu, W. Chen, *Biomaterials* **2008**, *29*, 2153.
34 H. Ajiro, J. Watanabe, M. Akashi, *Biomacromolecules* **2008**, *9*, 426.
35 H. Wada, Y. Tanaka, *Europhys. Lett.* **2009**, *87*, 58001.
36 S. Liang, L. Liu, Q. Huang, K. L. Yam, *Carbohydr. Polym.* **2009**, *77*, 718.
37 X. Zhang, X. Guo, S. Yang, S. Tan, X. Li, H. Dai, X. Yu, X. Zhang, N. Weng, B. Jian, J. Xu, *J. Appl. Polym. Sci.* **2009**, *112*, 3063.
38 T. Dai, X. Qing, H. Zhou, C. Shen, J. Wang, Y. Lu, *Synth. Met.* **2010**, *160*, 791.
39 S. Tian, G. Shan, L. Wang, *Acta Polym. Sin.* **2010**, *5*, 556.
40 S. Tian, G. Shan, L. Wang, *Acta Polym. Sin.* **2010**, *10*, 1175.
41 D. J. Waters, K. Engberg, R. Parke-Houben, C. N. Ta, A. J. Jackson, M. F. Toney, C. W. Frank, *Macromolecules* **2011**, *44*, 5776.
42 X. Wang, H. Wang, H. R. Brown, *Soft Matter* **2011**, *7*, 211.
43 Q. Zhao, J. Sun, X. Wu, Y. Lin, *Soft Matter* **2011**, *7*, 4284.
44 X. Wang, W. Hong, *Soft Matter* **2011**, *7*, 7960.
45 H. Tsukeshiba, M. Huang, Y.-H. Na, T. Kurokawa, R. Kuwabara, Y. Tanaka, H. Furukawa, Y. Osada, J. P. Gong, *J. Phys. Chem. B* **2005**, *109*, 16304.
46 D. Myung, D. Waters, M. Wiseman, P.-E. Duhamel, J. Noolandi, C. N. Ta, C. W. Frank, *Polym. Adv. Technol.* **2008**, *19*, 647.
47 O. E. Philippova, R. Rulkens, B. I. Kovtunenko, S. S. Abramchuk, A. R. Khokhlov, G. Wegner, *Macromolecules* **1998**, *31*, 1168.
48 M. Huang, H. Furukawa, Y. Tanaka, T. Nakajima, Y. Osada, J. P. Gong, *Macromolecules* **2007**, *40*, 6658.
49 T. Nakajima, H. Furukawa, Y. Tanaka, T. Kurokawa, Y. Osada, J. P. Gong, *Macromolecules* **2009**, *42*, 2184.
50 Y. Tanaka, R. Kuwabara, Y.-H. Na, T. Kurokawa, J. P. Gong, Y. Osada, *J. Phys. Chem. B* **2005**, *109*, 11559.
51 Y.-H. Na, Y. Tanaka, Y. Kawauchi, H. Furukawa, T. Sumiyoshi, J. P. Gong, Y. Osada, *Macromolecules* **2006**, *39*, 4641.
52 Y. Kawauchi, Y. Tanaka, H. Furukawa, T. Kurokawa, T. Nakajima, Y. Osada, J. P. Gong, *J. Phys.: Conf. Ser.* **2009**, *184*, 012016.
53 Q. M. Yu, Y. Tanaka, H. Furukawa, T. Kurokawa, J. P. Gong, *Macromolecules* **2009**, *42*, 3852.
54 Y. Tanaka, Y. Kawauchi, T. Kurokawa, H. Furukawa, T. Okajima, J. P. Gong, *Macromol. Rapid Commun.* **2008**, *29*, 1514.
55 R. E. Webber, C. Creton, H. R. Brown, J. P. Gong, *Macromolecules* **2007**, *40*, 2919.
56 Y. Tanaka, *Europhys. Lett.* **2007**, *78*, 56005.
57 Y.-H. Na, T. Kurokawa, Y. Katsuyama, H. Tsukeshiba, J. P. Gong, Y. Osada, S. Okabe, T. Karino, M. Shibayama, *Macromolecules* **2004**, *37*, 5370.
58 S. Liang, Z. L. Wu, J. Hu, T. Kurokawa, Q. M. Yu, J. P. Gong, *Macromolecules* **2011**, *44*, 3016.
59 H. R. Brown, *Macromolecules* **2007**, *40*, 3815.
60 G. E. Fantner, T. Hassenkam, J. H. Kindt, J. C. Weaver, H. Birkedal, L. Pechenik, J. A. Cutroni, G. A. G. Cidade, G. D. Stucky, D. E. Morse, P. K. Hansma, *Nat. Mater.* **2005**, *4*, 612.
61 D. Kaneko, T. Tada, T. Kurokawa, J. P. Gong, Y. Osada, *Adv. Mater.* **2005**, *17*, 535.
62 K. Yasuda, J. P. Gong, Y. Katsuyama, A. Nakayama, Y. Tanabe, E. Kondo, M. Ueno, Y. Osada, *Biomaterials* **2005**, *26*, 4468.
63 C. Azuma, K. Yasuda, Y. Tanabe, H. Taniguro, F. Kanaya, A. Nakayama, Y. M. Chen, J. P. Gong, Y. Osada, *J. Biomed. Mater. Res., Part A* **2006**, *81A*, 373.
64 K. Arakaki, N. Kitamura, T. Kurokawa, S. Onodera, F. Kanaya, J. P. Gong, K. Yasuda, *J. Mater. Sci.: Mater. Med.* **2011**, *22*, 417.
65 R. H. Baughman, C. Cui, A. A. Zakhidov, Z. Iqbal, J. N. Barisci, G. M. Spinks, G. G. Wallace, A. Mazzoldi, D. De Rossi, A. G. Rinzler, O. Jaschinski, S. Roth, M. Kertesz, *Science* **1999**, *284*, 1340.

66 M.-H. Li, P. Keller, J. Yang, P.-A. Albouy, *Adv. Mater.* **2004**, *16*, 1922.
67 Y. Bar-Cohen, *Electroactive Polymer (EAP) Actuators as Artificial Muscles: Reality, Potential and Challenges*, SPIE Press, Bellingham, **2004**.
68 Z. Liu, P. Calvert, *Adv. Mater.* **2000**, *12*, 288.
69 J. Fehér, G. Filipcsei, J. Szalma, M. Zrínyi, *Colloids Surf., A* **2001**, *183–185*, 505.
70 S. Liang, J. Xu, L. Weng, L. Zhang, X. Guo, X. Zhang, *J. Phys. Chem. B* **2007**, *111*, 941.
71 S. Liang, Q. M. Yu, H. Yin, Z. L. Wu, T. Kurokawa, J. P. Gong, *Chem. Commun.* **2009**, 7518.
72 T. Sadamoto, F. Bonde-Petersen, Y. Suzuki, *Eur. J. Appl. Physiol. Occup. Physiol.* **1983**, *51*, 395.
73 M. Long, H. J. Rack, *Biomaterials* **1998**, *19*, 1621.
74 C. Piconi, W. Burger, H. G. Richter, A. Cittadini, G. Maccauro, V. Covacci, N. Bruzzese, G. A. Ricci, E. Marmo, *Biomaterials* **1998**, *19*, 1489.
75 H. Ohgushi, N. Kotobuki, H. Funaoka, H. Machida, M. Hirose, Y. Tanaka, Y. Takakura, *Biomaterials* **2005**, *26*, 4654.
76 K. Messner, J. Gao, *J. Anat.* **1998**, *193*, 161.
77 T. Kurokawa, H. Furukawa, W. Wang, Y. Tanaka, J. P. Gong, *Acta Biomater.* **2010**, *6*, 1353.
78 J. Saito, H. Furukawa, T. Kurokawa, R. Kuwabara, S. Kuroda, J. Hu, Y. Tanaka, J. P. Gong, N. Kitamura, K. Yasuda, *Polym. Chem.* **2011**, *2*, 575.
79 A. G. Peressadko, N. Hosoda, B. N. J. Persson, *Phys. Rev. Lett.* **2005**, *95*, 124301.
80 B. N. J. Persson, O. Albohr, C. Creton, V. Peveri, *J. Chem. Phys.* **2004**, *120*, 8779.
81 J. J. Sahlin, N. A. Peppas, *J. Biomater. Sci., Polym. Ed.* **1997**, *8*, 421.
82 T. Nakajima, N. Takedomi, T. Kurokawa, H. Furukawa, J. P. Gong, *Polym. Chem.* **2010**, *1*, 693.
83 P. Giusti, L. Lazzeri, N. Barbani, P. Narducci, A. Bonaretti, M. Palla, L. Lelli, *J. Mater. Sci.: Mater. Med.* **1993**, *4*, 538.
84 K. Haraguchi, H.-J. Li, *Macromolecules* **2006**, *39*, 1898.
85 J. Hu, K. Hiwatashi, T. Kurokawa, S. M. Liang, Z. L. Wu, J. P. Gong, *Macromolecules* **2011**, *44*, 7775.
86 L. P. Gartner, J. L. Hiatt, *Color Textbook of Histology*, 2nd ed., Saunders, Philadelphia, **2001**.
87 S. Zhang, *Nat. Biotechnol.* **2003**, *21*, 1171.
88 C. Sanchez, H. Arribart, M. M. Giraud Guille, *Nat. Mater.* **2005**, *4*, 277.
89 Y. Kang, J. J. Walish, T. Gorishnyy, E. L. Thomas, *Nat. Mater.* **2007**, *6*, 957.
90 S. Zhang, M. A. Greenfield, A. Mata, L. C. Palmer, R. Bitton, J. R. Mantei, C. Aparicio, M. O. de la Cruz, S. I. Stupp, *Nat. Mater.* **2010**, *9*, 594.
91 Z. L. Wu, H. Furukawa, W. Yang, J. P. Gong, *Adv. Mater.* **2009**, *21*, 4696.
92 Y. Gao, F. Zhao, Q. Wang, Y. Zhang, B. Xu, *Chem. Soc. Rev.* **2010**, *39*, 3425.
93 S. Hestrin, M. Schramm, *Biochem. J.* **1954**, *58*, 345.
94 Y. Numata, K. Muromoto, H. Furukawa, J. P. Gong, K. Tajima, M. Munekata, *Polym. J.* **2009**, *41*, 524.
95 A. Nakayama, A. Kakugo, J. P. Gong, Y. Osada, M. Takai, T. Erata, S. Kawano, *Adv. Funct. Mater.* **2004**, *14*, 1124.
96 Y. Hagiwara, A. Putra, A. Kakugo, H. Furukawa, J. P. Gong, *Cellulose* **2010**, *17*, 93.
97 T. Dobashi, M. Nobe, H. Yoshihara, T. Yamamoto, A. Konno, *Langmuir* **2004**, *20*, 6530.
98 M. Nobe, T. Dobashi, T. Yamamoto, *Langmuir* **2005**, *21*, 8155.
99 T. Dobashi, K. Furusawa, E. Kita, Y. Minamisawa, T. Yamamoto, *Langmuir* **2007**, *23*, 1303.
100 K. Furusawa, Y. Minamisawa, T. Dobashi, T. Yamamoto, *J. Phys. Chem. B* **2007**, *111*, 14423.
101 W. Yang, H. Furukawa, J. P. Gong, *Adv. Mater.* **2008**, *20*, 4499.
102 Z. L. Wu, T. Kurokawa, D. Sawada, J. Hu, H. Furukawa, J. P. Gong, *Macromolecules* **2011**, *44*, 3535.
103 Z. L. Wu, D. Sawada, T. Kurokawa, A. Kakugo, W. Yang, H. Furukawa, J. P. Gong, *Macromolecules* **2011**, *44*, 3542.
104 K. Murata, K. Haraguchi, *J. Mater. Chem.* **2007**, *17*, 3385.
105 Z. L. Wu, T. Kurokawa, S. Liang, H. Furukawa, J. P. Gong, *J. Am. Chem. Soc.* **2010**, *132*, 10064.
106 Z. L. Wu, M. Arifuzzaman, T. Kurokawa, H. Furukawa, J. P. Gong, *Soft Matter* **2011**, *7*, 1884.
107 R. P. Wool, *Soft Matter* **2008**, *4*, 400.
108 Q. Wang, J. L. Mynar, M. Yoshida, E. Lee, M. Lee, K. Okuro, K. Kinbara, T. Aida, *Nature* **2010**, *463*, 339.
109 A. B. South, L. A. Lyon, *Angew. Chem.* **2010**, *122*, 779.
110 N. Holten-Andersen, M. J. Harrington, H. Birkedal, B. P. Lee, P. B. Messersmith, K. Y. C. Lee, J. H. Waite, *Proc. Natl. Acad. Sci. U.S.A.* **2011**, *108*, 2651.
111 M. A. Haque, G. Kamita, T. Kurokawa, K. Tsujii, J. P. Gong, *Adv. Mater.* **2010**, *22*, 5110.
112 M. A. Haque, T. Kurokawa, G. Kamita, J. P. Gong, submitted to *Macromolecules*.

Zi Liang Wu graduated in Chemical Engineering from Zhejiang University (China) in 2003 and received his Master's degree in 2006 at East China University of Science and Technology (China). He obtained his Ph.D. in Biological Sciences under the supervision of Prof. Jian Ping Gong at Hokkaido University (Japan) in 2010. His Ph.D. work was mainly focused on the self-assembling structures of lyotropic liquid crystals in solutions and hydrogels. And then, he joined the group of Prof. Eugenia Kumacheva as a postdoctoral fellow at University of Toronto (Canada).

Takayuki Kurokawa graduated in polymer science from Hokkaido University, Japan in 2000. He received his Ph.D. for study on Effect of Polymer Dynamics on Friction of Gels from Hokkaido University in 2005. He joined RIKEN, Japan as a postdoctoral researcher, then Creative Research Institution at Hokkaido University as an assistant professor since 2009. He focuses on functions of polymer gels, such as mechanical property, permeability, and biological property.

Award recipient

Jian Ping Gong is the professor of Faculty of Advanced Life Science, Hokkaido University. She received her Bachelor's degree in physics from Zhejiang University, China, and her Master's degree in polymer science from Ibaraki University, Japan. She studied high T_c superconductors at Tokyo Institute of Technology where she gained her Doctor of Engineering. She joined the faculty at the Hokkaido University in 1993, where she received her Doctor of Science for the study of polyelectrolyte gels. She received Wiley Polymer Science Award (2001), The Award of the Society of Polymer Science Japan (2006), and The Chemical Society of Japan Award for Creative Work (2010). Gong served as the Chair of Executive Committee, The Research Group of Polymer Gel, Japan (2004–2005), and is serving as the board member of the Society of Polymer Science, Japan. She also serves on the editorial and advisory boards of Soft Matter, Macromolecules, Biointerphases, and Asia Materials. Gong currently is concentrating on the researches of novel hydrogels with high mechanical performances, such as high toughness, low surface friction, shock-absorbing, self-healing, and the application of the hydrogels as biotissues.